Age-related increases in long-range connectivity in fetal functional neural connectivity networks *in utero*

Moriah E. Thomason [a,b,d,*], Lauren E. Grove [a,d], Tim A. Lozon Jr. [e],
Angela M. Vila [a], Yongquan Ye [f], Matthew J. Nye [g], Janessa H. Manning [a,d],
Athina Pappas [b,d], Edgar Hernandez-Andrade [d,h], Lami Yeo [d,h], Swati Mody [e],
Susan Berman [h], Sonia S. Hassan [d,h], Roberto Romero [c,d]

[a] Merrill Palmer Skillman Institute for Child and Family Development, Wayne State University, Detroit, MI 48202, USA
[b] Department of Pediatrics, Wayne State University School of Medicine, Detroit, MI 48202, USA
[c] Perinatology Research Branch, NICHD/NIH/DHHS, Bethesda, MD, USA
[d] Perinatology Research Branch, NICHD/NIH/DHHS, Detroit, MI 48202, USA
[e] Michigan State University School of Medicine, East Lansing, MI, 48824 USA
[f] Department of Radiology, Wayne State University School of Medicine, Detroit, MI 48202, USA
[g] University of Michigan School of Dentistry, Ann Arbor, MI 48109, USA
[h] Department of Obstetrics and Gynecology, Wayne State University School of Medicine, Detroit, MI 48202, USA

ARTICLE INFO

ABSTRACT

Formation of operational neural networks is one of the most significant accomplishments of human fetal brain growth. Recent advances in functional magnetic resonance imaging (fMRI) have made it possible to obtain information about brain function during fetal development. Specifically, resting-state fMRI and novel signal covariation approaches have opened up a new avenue for non-invasive assessment of neural functional connectivity (FC) before birth. Early studies in this area have unearthed new insights about principles of prenatal brain function. However, very little is known about the emergence and maturation of neural networks during fetal life. Here, we obtained cross-sectional rs-fMRI data from 39 fetuses between 24 and 38 weeks postconceptual age to examine patterns of connectivity across ten neural FC networks. We identified primitive forms of motor, visual, default mode, thalamic, and temporal networks in the human fetal brain. We discovered the first evidence of increased long-range, cerebral-cerebellar, cortical-subcortical, and intra-hemispheric FC with advancing fetal age. Continued aggregation of data about fundamental neural connectivity systems *in utero* is essential to establishing principles of connectomics at the beginning of human life. Normative data provides a vital context against which to compare instances of abnormal neurobiological development.

1. Introduction

One of the major achievements of human fetal brain development is the establishment of functional neural networks. Detailed understanding of normal processes of brain circuit formation is essential for discovering consequences of injury/insult, periods of vulnerability, and for early detection of clinically significant neural anomalies.

* Corresponding author at: Merrill Palmer Skillman Institute, 71 E. Ferry Street, Detroit, MI 48202, USA. Tel.: +1 313 664 2517; fax: +1 313 664 2555.
  E-mail address: moriah@wayne.edu (M.E. Thomason).

The bulk of what is known about human brain connectional ontogeny comes from histological and magnetic resonance imaging (MRI) studies performed on post-mortem fetal brain specimens. These histological and MRI studies have shown that transient physical structures serve as scaffolding for axonal proliferation and cell migration (Kostovic and Jovanov-Milosevic, 2008) and that, in harmony with brain gyrification, long-range association pathways begin to be established during the second half of gestation (Kostović and Jovanov-Milosevic, 2006; Takahashi et al., 2012).

Until recently, quantification of neuroconnectivity during the fetal period has proven elusive for human *in vivo* brain research. However, recent advances in diffusion and resting state MRI have provided new means for non-invasive study of neural circuit formation in the perinatal period (Mailath-Pokorny et al., 2012). Tractography analyses of fetal brain diffusion tensor imaging data has demonstrated emergence of white matter pathways in the transient intermediate zone, splenium, and genu, consistent with *in vitro* findings (Kasprian et al., 2008). Resting-state functional MRI (rs-fMRI) applied to prematurely born human infants has shown that, as the preterm neonate grows, neural circuit functional activity becomes increasingly synchronized (Smyser et al., 2010) and that intrinsic connectivity networks (ICNs) are largely formed by 42 weeks postmenstrual age (Doria et al., 2010). However, preterm neonates are not ideal substitutes for learning about typical fetal brain development, because the underlying reason for preterm delivery and environmental factors cannot be disentangled from neurological observations in these cases. Important questions remain about large-scale neural organization, and establishment of ICNs prior to birth.

Recent investigations have established the utility of rs-fMRI for quantifying neural network development *in utero*. The first fetal rs-fMRI study was performed in pregnant women referred to MRI for suspected neurological anomalies discovered during fetal sonography. The investigators qualitatively compared functional connectivity (FC) networks in 16 fetuses that had healthy MRI results and minimal movement. They concluded that in the majority of cases temporal lobe networks were lateralized, whereas frontal and occipital networks were bilateral (Schöpf et al., 2012). Subsequently, two human fetal FC studies have been performed, assessing fetuses recruited as part of research studies, rather than as part of clinical follow-up. Statistical group-level comparisons of FC in 25 healthy fetuses demonstrated that cross-hemispheric connectivity increases with advancing postconceptual age, and that midline cross-hemispheric connectivity precedes lateral connectivity (Thomason et al., 2013). Graph theoretical analyses in 33 fetuses revealed that synchrony of activity across neural networks is increased in older, compared to younger, fetuses. In addition, connectivity between the posterior cingulate cortex (PCC) and other brain areas becomes more negative with increasing postconceptual age (Thomason et al., 2014). These studies provided the first indication that human fetuses possess basic forms of neural connectivity networks and that rs-fMRI may become instrumental for determining principals of human FC *in utero*.

Age-related changes in resting-state networks *in utero* remain unclear. We obtained cross-sectional rs-fMRI data from 39 fetuses between 24 and 38 weeks postconceptual age to examine patterns of connectivity across ten functionally integrated ICNs. Following prior work in neonates (Smyser et al., 2010), we measured fMRI covariation in sensorimotor, cingulate, occipital, prefrontal, temporal, and thalamic regions. Employing seed-based connectivity analysis (SCA), we interrogated qualitative and quantitative changes in ICNs associated with advancing fetal age. We predicted that homotopic and long-range connectivity would be strongest in older fetuses, across neural networks, and that within network covariance would be higher and between network covariance would be lower in older fetuses. The latter would be fitting with emergence of independently functioning ICNs.

2. Methods

2.1. Participants

Rs-fMRI data were collected from healthy pregnant women and their fetuses recruited from obstetrical clinics located within the Detroit Medical Center. Initial contact was made by physicians to potential participants in their care and followed up by one-on-one discussion with a member of the research team who explained study procedures and answered questions. Participants were informed that their participation in research was voluntary and not part of their prenatal care. They were assured that they were not selected on the basis of any medical findings, and it was explained that their choice to participate would not influence their future medical care. Exclusionary criteria included: presence of MRI contraindication, fetal central nervous system abnormality, and maternal size larger than would comfortably be accommodated in a 70-cm open-bore MRI system. Inclusionary criteria included: singleton pregnancy between 24 and 38 weeks postconceptual age, and maternal age ≥18 years. Written, informed consent was obtained prior to participation. All experimental procedures were approved by the Human Investigation Committee of Wayne State University.

Data were collected from a total of 39 pregnant women (median maternal age = 23 years, range = 18–37 years). The median gestational age (GA) of their fetuses was 32 weeks (range = 24 + 4 to 37 + 6, weeks + days) at the time of MRI. Seven fetal participants were excluded prior to group level analyses due to (a) having fewer than 100 fMRI volumes after removing high movement frames ($n = 4$), or (b) because they went on to be born preterm ($n = 3$), leaving a total of 32 participants. fMRI data from 22 of these participants has been reported previously (Thomason et al., 2014, 2013).

2.2. Measures

Information about maternal health practices were obtained using a 45-item health questionnaire which assessed frequency of engaging in specific health behaviors related to diet, exercise, medical adherence, alcohol and tobacco use and exposure, and sleep (adapted from Jackson,

2006). Supplementary Table S1 provides a summary of questionnaire items. Health practices and birth outcomes (*e.g.*, newborn weight, height, head circumference) were compared between younger ($\bar{x} = 27.55$ weeks, SD ± 1.49), middle ($\bar{x} = 32.84$ weeks, SD ± 1.97) and older ($\bar{x} = 36.05$ weeks, SD ± 0.85) fetal groups by analysis of variance (ANOVA) implemented in SPSS version 21; $p \leq 0.05$ was considered significant.

2.3. Imaging methods

Fetal MR exams were performed with a Siemens Verio 70-cm open-bore 3 Tesla scanner. An abdominal 4-Channel Siemens Flex Coil was placed around the maternal abdomen centered approximately at the fetal head. A T2 HASTE anatomical sequence (TR/TE, 3500/140 ms; 3-mm slice thickness) was repeated six times, twice in each orientation. Echo planar imaging (EPI) BOLD (TR/TE, 2000/30 ms; 4-mm slice thickness; axial) was performed for variable duration to accommodate readjustments to acquisition following fetal movement. The average number of BOLD fMRI time frames obtained per case was 349 (SD = 70). Specific absorption rates were extracted from fMRI scans for every subject.

2.4. Functional data preprocessing

BrainSuite (Shattuck and Leahy, 2002), Analyze 11.0 (AnalyzeDirect), and FSLview (Smith et al., 2004) were used to manually extract the fetal brain from surrounding tissue. Because the fetus is encased in an independently moving compartment (*e.g.*, the mother), the fetal brain must be manually extracted before standard motion realignment procedures can be employed. As manual brain extraction is time intensive (requiring generation of masks *via* manual tracing) we extracted only frames during which fetal movement was minimal (mean duration = 74.41 s, SD = 53.632 s; min = 20 s, max = 338 s). Frame selection determinations were made after repeatedly viewing the timeseries as a movie in FSLview. Each segment during which fetal head movement was minimal was manually segmented from surrounding maternal and skull tissue, reoriented, realigned, and normalized to a 32-week fetal template (Serag et al., 2012) using Statistical Parametric Mapping version 8 (SPM8). The 32-week fetal template was selected as it was closest to the mean fetal GA. To correct for variations in normalization between segments, normalized images were then concatenated into one run, realigned, and a 6 mm full width half max (FWHM) Gaussian smoothing kernel was applied.

To evaluate possible covariation between fetal age and data quality, movement and number of analyzed time frames were compared in fetuses of different ages. Movement parameters were computed for both translational (T_x, T_y, T_z in mm) and rotational (R_{pitch}, R_{roll}, R_{yaw} in degrees) movement, including (a) mean movement, (b) the mean of the maximum frame-to-frame displacement across the data, or max excursion, and (c) the mean of the standard deviation for all frames after linear detrending, or root mean square (RMS). Thus, a total of 18 movement parameters were utilized to quantify fetal head movement.

Table 1
Seed correlation maps were formed by correlating timecourse in each of these coordinate regions with all voxels in the brain.

Intrinsic Connectivity Network (ICN)	32-week fetal template coordinates, Serag et al. (2012)		
	X	Y	Z
Motor leg	12	−6	26
Motor hand	24	0	20
Motor face	30	4	10
Caudal posterior cingulate cortex	4	−20	0
Dorsal anterior cingulate cortex	2	24	4
Cuneus	6	−38	−8
Medial prefrontal cortex	2	36	−10
Lateral prefrontal cortex	20	38	−10
Superior temporal gyrus	32	0	−4
Dorsal thalamus	4	0	−2

Additionally, the number of frames retained for all subjects was restricted to within 2 standard deviations (SD ± 50 frames) of the sample mean ($\bar{x} = 200$). To test whether fetal age related to estimated differences in movement-related error or to number of frames analyzed ANOVA and bivariate Pearson correlation were implemented in SPSS version 21; $p \leq 0.05$ was considered significant.

2.5. Functional connectivity analyses

A seed-based connectivity approach implemented in CONN-fMRI toolbox ver.12.k (Whitfield-Gabrieli and Nieto Castanon, 2012) was utilized to compute connection values between spontaneous fMRI signal in a 6 mm radius "seed" (source) region and all other brain voxels. FC analyses were performed for 10 seed regions approximating anatomical areas previously tested in a study of preterm and term newborns (Smyser et al., 2010). Seed based connectivity analyses were performed in standardized space. Coordinates for seed regions are provided in Table 1, and illustrated in Fig. 1. Anatomical component correction (aCompCor) methodology, rather than global signal correction, was used to estimate and remove noise at the individual voxel level (Behzadi et al., 2007; Chai et al., 2012). In the present analysis we did not apply global signal correction because of the concern that it forces the presence of anticorrelated networks (Chang and Glover, 2009; Murphy et al., 2009; Weissenbacher et al., 2009), which could lead to false interpretation of observed effects. Principal components of the signals from white matter and cerebral spinal fluid, as well as translational and rotational movement parameters (and their first-order temporal derivatives) were removed by covariate regression analysis. A temporal band-pass filter of 0.01–0.1 Hz was applied to investigate low frequency correlations. Individual volume images resulting from seed-based connectivity analyses were submitted to random effects modeling in SPM8. One sample *t*-tests and linear regression were performed to obtain qualitative comparisons of networks in different fetal age groups and to quantify significant age-related changes in FC, respectively. Statistical tests assumed unequal variance. All neuroimaging results were considered significant at $p \leq 0.01$.
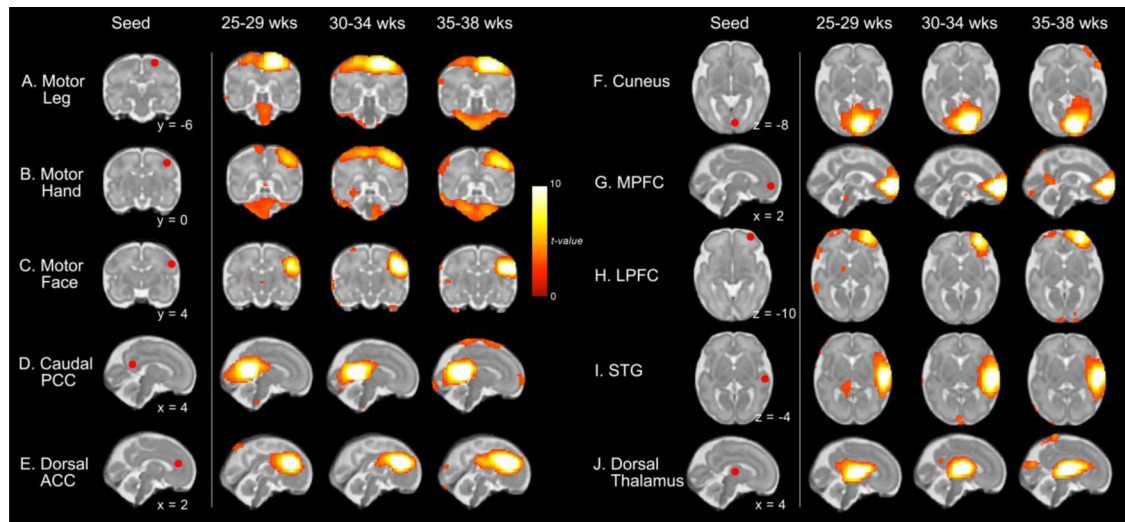
Fig. 1. *In utero* whole-brain resting-state correlation maps corresponding to varied seed locations. Images are organized into columns corresponding to fetal age groups. Seed regions are shown in the first column on the left. Age-group 1-sample *t*-tests at *p* < 0.01 significance threshold are shown on representative coronal, sagittal, and axial slices overlaid on a 32-week fetal template (Serag et al., 2012). *Abbreviations*: posterior cingulate cortex, PCC; anterior cingulate cortex, ACC; medial prefrontal cortex, MPFC; lateral prefrontal cortex, LPFC; superior temporal gyrus, STG.

2.6. Analysis of age-related increases in long-range connectivity

We quantitatively examined the relationship between fetal age and amount of significant distant connectivity. Distant was defined as the furthest 2% of significant voxels (on average > 63 mm), specified individually for each of the 10 networks to accommodate their inherent unique spatial distributions. Sums of the number of distant voxels with *t*-values >2.462 (corresponding to $p \leq 0.01$) were submitted to a between-groups ANOVA implemented in SPSS version 21; $p \leq 0.01$ was considered significant.

3. Results

3.1. Participant characteristics

Participant and data characteristics across fetuses of different ages are summarized in Table 2. Fetal age groups did not differ in (1) self-reported health practices, $F(2,28) = 0.047$, $p = 0.96$, (2) number of retained fMRI time frames, $\bar{x} = 200$, SD ± 50, $F(2,29) = 0.902$, $p = 0.42$, (3) specific absorption rates during fMRI, $\bar{x} = 0.241$ W/kg, SD ± 0.09, $F(2,29) = 0.664$, $p = 0.52$, nor (4) any of the 18 evaluated movement parameters (see supplementary

Table S2). All fetuses included in analyses were delivered at term, and none were hospitalized following delivery.

3.2. Increased neural network connectivity in older fetuses

Voxel-wise group regression revealed increased functional connectivity in older compared with younger fetuses in 7 of the 10 networks examined (networks A, B, C, F, H, I, J; all *p* < 0.01, cluster extent, *k* > 10). Motor, visual, auditory and thalamic networks showed overall increased FC with age, whereas midline connectivity networks (anterior and posterior cingulate and medial PFC) showed increased FC in younger fetuses.

3.3. Establishment of motor networks in utero

Patterns of motor, thalamic, and cerebellar connectivity varied in fetuses of different ages. Stronger FC was observed in older fetuses between motor cortices and thalamus and motor cortices and contralateral cerebellum, as illustrated in Fig. 2. In line with increased maturation of motor systems *in utero*, we also observed increased signal covariation between right and left primary motor cortices. This increased cross-hemispheric synchrony with increased age

Table 2
Summary of participant and data characteristics.

	N (M:F)	GA at MRI (wks)	Birth Measures					Frame total
		Mean (SD)	GA at birth (wks) Mean (SD)	Weight (g) Mean (SD)	Length (cm) Mean (SD)	HC (cm) Mean (SD)	5 min Apgar Median (IQR)	Mean (SD)
Youngest	11 (7:4)	27.5 (1.5)	38.7 (0.7)	3107.7 (397.7)	49.4 (2.6)	33.9 (2.0)	9 (0)	193.8 (55.4)
Middle	10 (6:4)	32.8 (2.0)	39.2 (1.1)	3549.9 (508.9)	51.0 (2.5)	34.3 (1.4)	9 (0)	217.4 (40.2)
Oldest	11 (6:5)	36.1 (0.9)	39.1 (1.1)	3051.1 (604.8)	48.5 (3.7)	33.1 (2.1)	9 (0)	190.4 (51.6)
Overall	32 (19:13)	32.2 (3.9)	39.0 (0.7)	3226.4 (542.1)	49.6 (3.1)	33.8 (1.9)	9 (0)	200.0 (49.6)

Abbreviations: male, M; female, F; standard deviation, SD; gestational age, GA; weeks, wks; grams, g; centimeters, cm; intraquartile range, IQR.
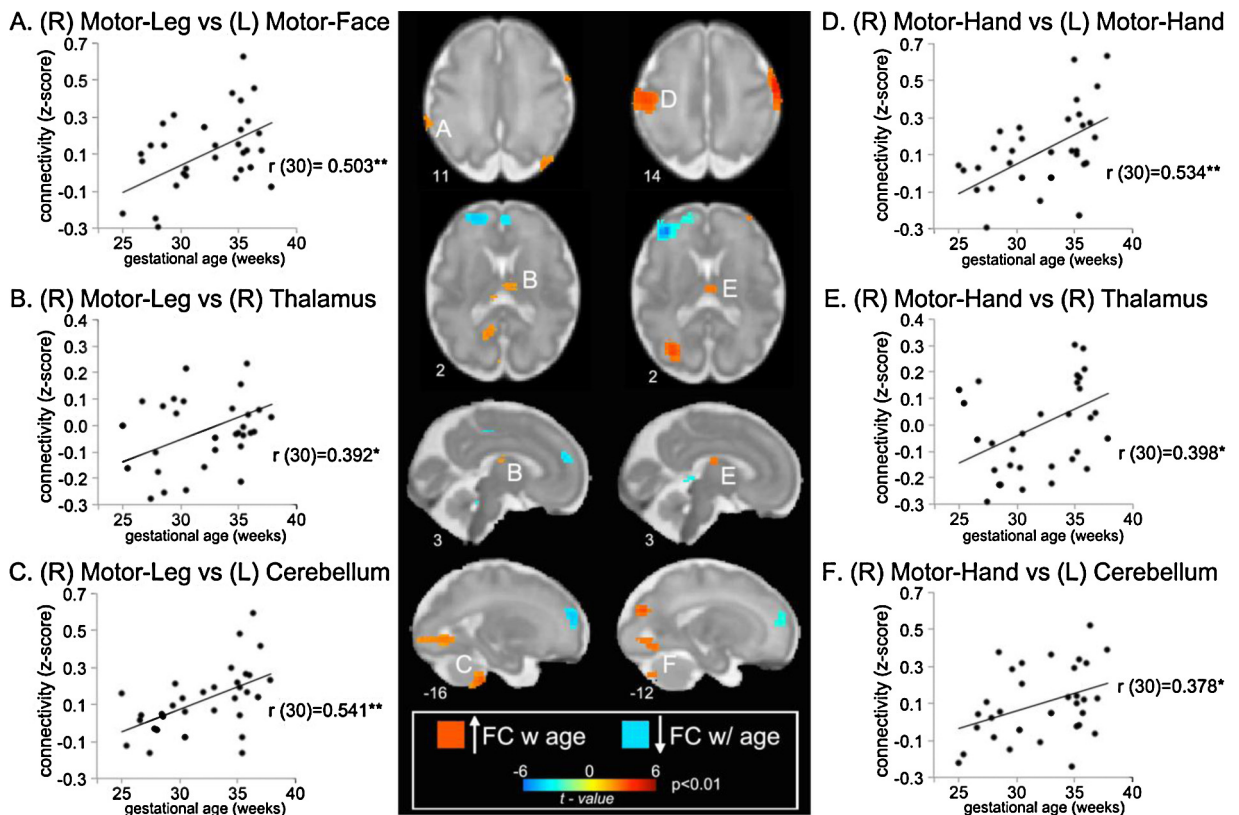
Fig. 2. Whole-brain fetal age regression analyses for Motor-Leg and Motor-Hand regions given on figure left and right side, respectively. Sagittal and axial slices at intersections of significant results for each regression are overlaid on 32-week fetal templates. Coordinates for each image are given in mm at the bottom left of each slice. Scatterplots depict functional connectivity (*i.e.*, signal covariation) plotted as Fisher's transformed r values between specified, lettered brain areas and motor cortex across participants. With age, functional connectivity increased between bilateral motor regions, between motor cortices and ipsilateral thalamic regions, and between motor cortices and contralateral cerebellar regions. $^*p \leq 0.05$; $^{**}p \leq 0.01$.

effect was strongest in the motor hand, compared to the motor face and motor leg networks.

3.4. Increased FC in default mode network (DMN) components in older fetuses

Qualitative comparisons of statistical results obtained in each fetal age group revealed significant caudal PCC to medial prefrontal connectivity was present in the oldest but not the younger fetal groups. This is portrayed in Fig. 1, which shows significant patterns of connectivity in each age group. The oldest fetal group demonstrated positive connectivity from the PCC seed to MPFC (Fig. 1, row D) and the reverse, MPFC seed to the PCC (Fig. 1, row G). These regions are key contributors to the DMN of the brain. Activity in the DMN has been shown to be reduced when individuals engage in attentionally demanding tasks, and activity in this network is negatively correlated with increased activity in regions important for executive function such as lateral prefrontal and parietal association cortices (Fox et al., 2005). Linear regression of fetal caudal PCC maps revealed that both positive connectivity to MPFC and negative connectivity to lateral prefrontal/parietal regions are increased in older fetuses (see Fig. 3).

3.5. Greater long-range connectivity in older fetuses

Older fetuses had significantly more long-range connectivity than younger fetuses, $F(2,29) = 5.873$, $p = 0.008$. Averages of total number of distant (furthest 2%) connected voxels revealed the youngest group had fewest ($\bar{x} = 416$), the middle age group was intermediate ($\bar{x} = 784$), and the oldest group had largest number of distant suprathreshold voxels ($\bar{x} = 1549$). This difference between groups showed some variation across networks, with strongest separation between age groups for the caudal PCC, cuneus, LPFC, motor-leg, and motor-hand networks, in that order. The number of significant distant voxels in the aforementioned networks was more than five times greater in older than younger fetal groups. Results are plotted individually for each network in Fig. 4. Given that these analyses were performed in standardized space, the observed age-group differences should not be attributed to variation in overall brain volume.

4. Discussion

The primary goals of this study were to determine if typical resting state ICNs are present in the human fetal brain before birth and how connectivity in these networks
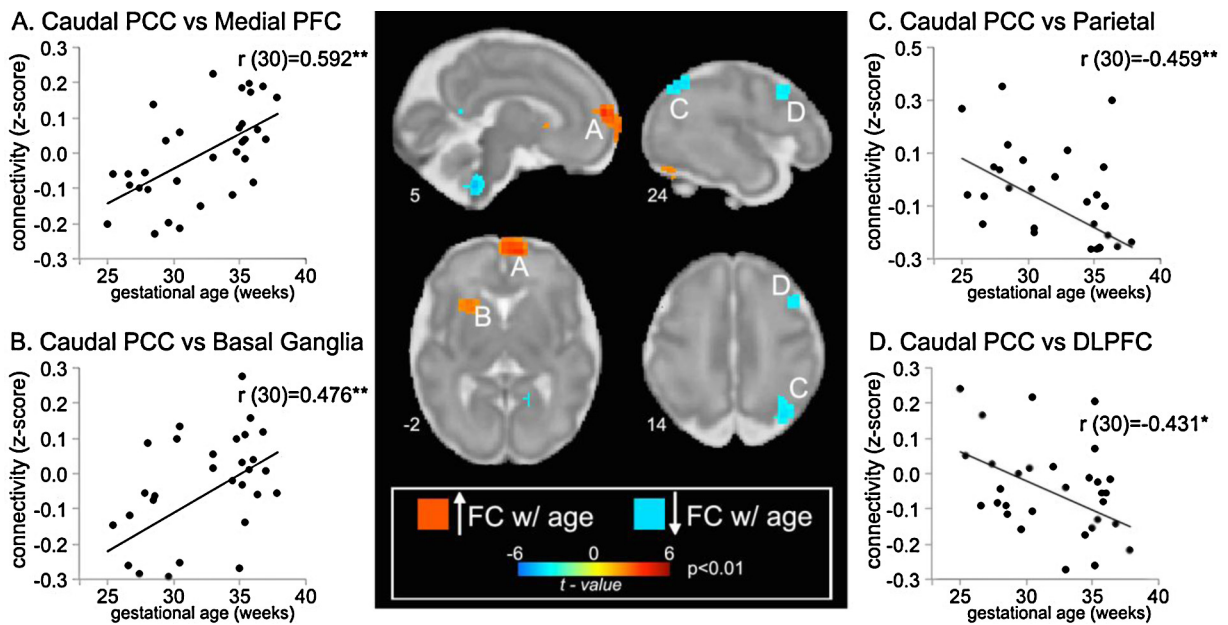
Fig. 3. Whole-brain fetal age regression analysis for the PCC seed region. Sagittal and axial slices at intersections of significant results are overlaid on 32-week fetal templates. Coordinates for each image are given in mm at the bottom left of each slice. Scatterplots depict functional connectivity (*i.e.*, signal covariation) plotted as Fisher's transformed r values between specified, lettered brain areas and the caudal PCC across participants. With age, functional connectivity increased from PCC to medial prefrontal cortex and basal ganglia but decreased to parietal association areas and dorsal lateral prefrontal cortex. $^{*}p \leq 0.05$; $^{**}p \leq 0.01$.

varies with fetal age. Consistent with our hypotheses, we found that in older fetuses (1) long-range connectivity is stronger, (2) connectivity within ICNs is stronger, and (3) connectivity to areas outside of ICNs is reduced. For example, coactivation within motor, thalamic, and contralateral cerebellar regions increased with postconceptual age. These phenomena presumably reflect ongoing refinement within and between neural circuits, fitting with well described principals of neural segregation (Friston, 2002), and reproducing patterns observed in transitions from childhood to adulthood (Fair et al., 2007; Stevens et al., 2009).

We observed that older fetuses possess more significant long-range connections across networks. The principal of stronger long-range neural connections with advancing age has been demonstrated previously in neonates (Fransson et al., 2007; Gao et al., 2009), and across childhood and adolescence (Fair et al., 2007, 2009; Hagmann et al., 2010; Kelly et al., 2009; Supekar et al., 2009). Here, we show that this age related refinement in neural network architecture is present and observable beginning in the fetal period. Increased long-range signal covariance in older fetuses is fitting with prior observations that long-range association pathways form prenatally (Kostović and Jovanov-Milosevic, 2006; Takahashi et al., 2012). We advance these priors by demonstrating these effects in an *in vivo* model that will permit future examinations of health, injury, and disease etiology in fetal life.

Functional connections between regions most commonly cited as comprising the DMN, the PCC and medial PFC, were evident in fetuses older than 35 weeks postconceptual age. Coactivation of PCC and medial PFC became

more synchronized with age, while coactivation from the PCC to areas of dorsal attention/executive networks became more negatively coupled with age. This is in agreement with previous graph theoretical resting-state fMRI in human fetuses showing that older (GA ≥ 31 weeks) but not younger fetuses (GA < 31 weeks) exhibit a module, or connectivity subnetwork, that comprises dorsal posterior and medial frontal brain regions (Thomason et al., 2014). That study also demonstrated that negative connectivity between the PCC and other brain regions increases with fetal age (Thomason et al., 2014). Together these unique approaches provide convergent support that regions of the DMN manifest distinctly coordinated activity prior to birth. Discovering coordinated DMN function *in utero* is also consistent with studies in term- and preterm-born infants where a 'proto-default-mode network' has been indicated (Fransson et al., 2007, 2009).

Here, we discovered that temporal coherence in human fetal fMRI signals extends beyond synchrony in homotopic counterparts. Indeed, we observed several temporal coherence patterns: (1) subcortical to cortical (*e.g.*, motor cortices to thalamic regions), (2) intra- (*e.g.*, PCC to medial PFC) and inter-hemispheric (*e.g.*, bilateral PFC and motor cortices), and (3) cerebral to cerebellar (*e.g.*, motor cortices to contralateral cerebellum). Synchrony in fMRI signal can occur in the absence of direct anatomical connection (Greicius et al., 2009; Vincent et al., 2007). However, studies of adults with acute stroke (Lv et al., 2013), a child with a severed corpus callosum (Johnston et al., 2008), and combined diffusion tensor-FC studies (Greicius et al., 2009) indicate fMRI signal covariation is constrained by physical structures of the brain. Therefore, it has been suggested that
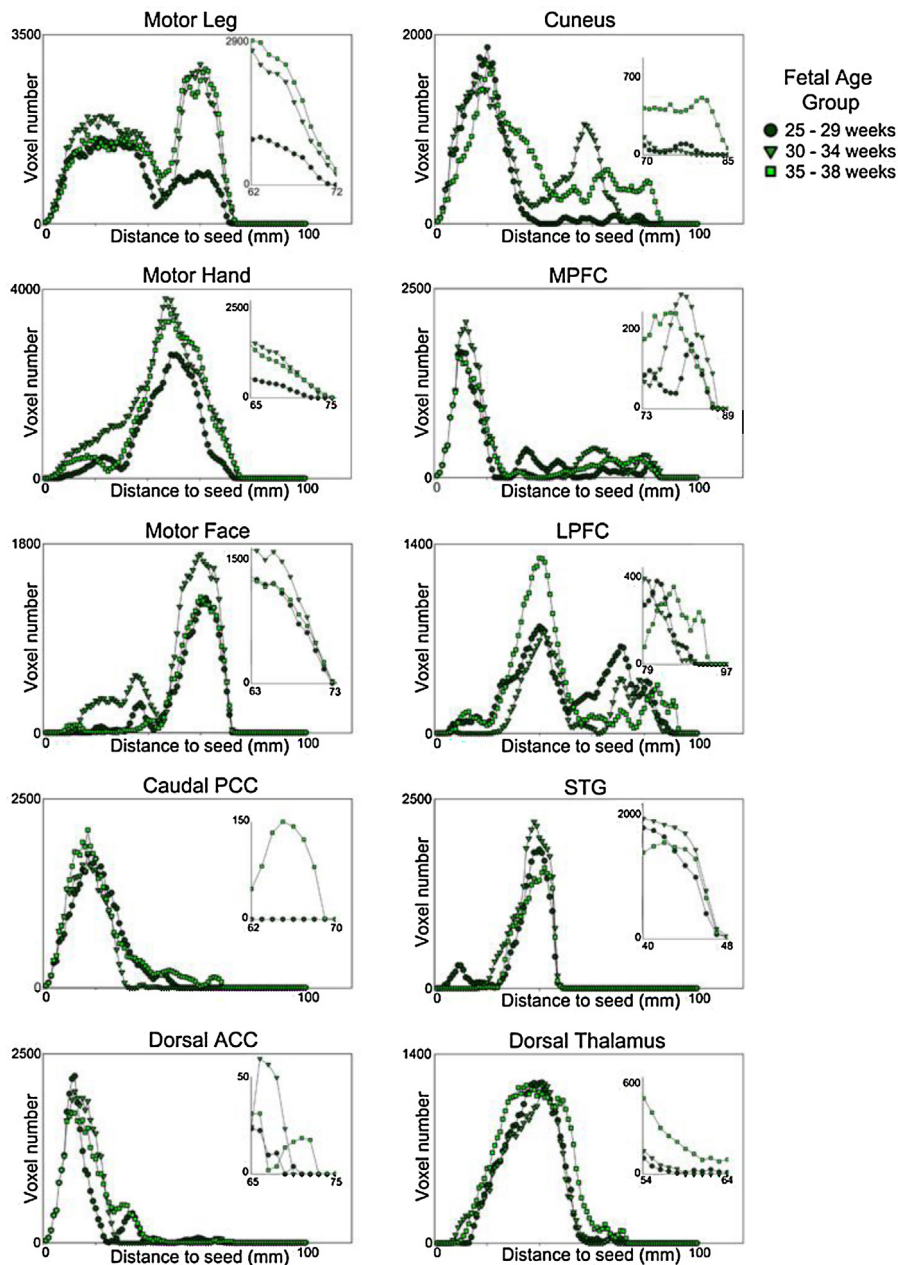
Fig. 4. Number of suprathreshold voxels plotted against distance from seed coordinate. The relationship between distance to seed and number of significant voxels is shown for each of the three fetal age groups and for each network examined. Inset plots magnify select distant ranges to provide enhanced visualization of differences between groups.

resting-state signal correlations should be interpreted as reflecting histories of coactivation between brain regions (Dosenbach et al., 2007; Kelly et al., 2009; Power et al., 2010). In the human fetus this activity may represent active establishment of common function that emerges prior to the development of related cognitive or perceptual functions. This postulation is justified given extensive evidence that network dynamics can reshape the physical structures of neural networks (Katz and Shatz, 1996; Majewska and Sur, 2006). Here, we discovered many forms of network temporal coherence (*e.g.*, cerebellar to cerebral, subcortical

to cortical, homotopic) using fetal resting-state fMRI. Thus, spontaneous brain activity in the third trimester appears to recapitulate basic forms of human ICNs that may serve as scaffolding for development of these network structures.

A limitation to be considered in the present study is whether the seed regions selected for this study were ideal. There is limited precedence for coordinate selection in a fetal sample and a paucity of labeled fetal atlases or analyses tools available (Anderson and Thomason, 2013). Thus, for the present analysis, we adhered tightly to procedures successfully used in premature infants (Smyser

et al., 2010) as these best approximate neuroanatomy of our study sample. Another limitation of our study is that we evaluated only 10 *XYZ* coordinates (*i.e.*, seed regions) all located in the right hemisphere. This was an intentional constraint as we sought to restrict the total number of comparisons to reduce the possibility of introducing type I error (*i.e.*, false positives). By comparison, prior resting-state analyses in preterm infants have tested 5–30 seed regions and have used more relaxed significance thresholds (Doria et al., 2010; Smyser et al., 2010). A final significant concern to be considered in the present study is potential error introduced by fetal motion. Recent studies of the effects of motion on resting-state fMRI have shown that even 'micro-movement', as small as 0.2 mm, can impact observed patterns of functional connectivity (Power et al., 2012; Satterthwaite et al., 2013; Van Dijk et al., 2012). Disconcertingly, these investigations show that increased movement can falsely inflate short-range connectivity and decrease long-range connectivity. To mitigate movement related error, we excluded high motion frames across subjects, resulting in similar overall movement across age groups. By intentionally removing equivalent frame numbers in older and younger fetal groups we were also able to assure that fetal participants were matched on total number of frames analyzed. By controlling these variables across groups we limited concern that quality of neuroimaging data may influence observed effects.

5. Conclusions

Through resting-state evaluation of healthy human fetuses we have identified the earliest forms of neural functional connectivity. Motor, visual, thalamic, DMN, frontal, and temporal networks likely represent immature forms of those described in older populations. We observed temporal coherence across (1) cerebral-cerebellar, (2) cortical-subcortical, (3) intra-hemispheric cortical, and (4) bilateral, cross-hemispheric structures, suggesting many forms of cerebral connectivity are present by the third trimester. We also observed that older fetuses possess significantly more long-range connections than younger fetuses. By evaluating resting-state fMRI in healthy human fetuses we have gained new information about operations in functional brain circuits *in utero*. Continued development and use of fetal resting-state fMRI is likely to result in major discoveries for clinical, perinatal and neurological sciences.

Conflict of interest statement

All authors declare no competing financial interests.

Appendix A. Supplementary data

Supplementary data associated with this article can be found, in the online version, at http://dx.doi.org/10.1016/j.dcn.2014.09.001.

References

AnalyzeDirect, Overland Park, KS.

Anderson, A.L., Thomason, M.E., 2013. Functional plasticity before the cradle: a review of neural functional imaging in the human fetus. Neurosci. Biobehav. Rev. 37 (9), 2220–2232.

Behzadi, Y., Restom, K., Liau, J., Liu, T.T., 2007. A component based noise correction method (CompCor) for BOLD and perfusion based fMRI. Neuroimage 37 (1), 90–101.

Chai, X.J., Castanon, A.N., Ongur, D., Whitfield-Gabrieli, S., 2012. Anticorrelations in resting state networks without global signal regression. Neuroimage 59 (2), 1420–1428.

Chang, C., Glover, G.H., 2009. Effects of model-based physiological noise correction on default mode network anti-correlations and correlations. Neuroimage 47 (4), 1448–1459.

Doria, V., Beckmann, C.F., Arichi, T., Merchant, N., Groppo, M., Turkheimer, F.E., et al., 2010. Emergence of resting state networks in the preterm human brain. Proc. Natl. Acad. Sci. U.S.A. 107 (46), 20015–20020.

Dosenbach, N.U., Fair, D.A., Miezin, F.M., Cohen, A.L., Wenger, K.K., Dosenbach, R.A., et al., 2007. Distinct brain networks for adaptive and stable task control in humans. Proc. Natl. Acad. Sci. U.S.A. 104 (26), 11073–11078.

Fair, D.A., Cohen, A.L., Power, J.D., Dosenbach, N.U., Church, J.A., Miezin, F.M., et al., 2009. Functional brain networks develop from a "local to distributed" organization. PLoS Comput. Biol. 5 (5), 1–14.

Fair, D.A., Dosenbach, N.U.F., Church, J.A., Cohen, A.L., Brahmbhatt, S., Miezin, F.M., et al., 2007. Development of distinct control networks through segregation and integration. Proc. Natl. Acad. Sci. U.S.A. 104 (33), 13507–13512.

Fox, M.D., Snyder, A.Z., Vincent, J.L., Corbetta, M., Van Essen, D.C., Raichle, M.E., 2005. The human brain is intrinsically organized into dynamic, anticorrelated functional networks. Proc. Natl. Acad. Sci. U.S.A. 102 (27), 9673–9678.

Fransson, P., Skiold, B., Engstrom, M., Hallberg, B., Mosskin, M., Aden, U., et al., 2009. Spontaneous brain activity in the newborn brain during natural sleep – an fMRI study in infants born at full term. Pediatr. Res. 66 (3), 301–305.

Fransson, P., Skiold, B., Horsch, S., Nordell, A., Blennow, M., Lagercrantz, H., et al., 2007. Resting-state networks in the infant brain. Proc. Natl. Acad. Sci. U.S.A. 104 (39), 15531–15536.

Friston, K., 2002. Functional integration and inference in the brain. Prog. Neurobiol. 68 (2), 113–143.

Gao, W., Zhu, H., Giovanello, K.S., Smith, J.K., Shen, D., Gilmore, J.H., et al., 2009. Evidence on the emergence of the brain's default network from 2-week-old to 2-year-old healthy pediatric subjects. Proc. Natl. Acad. Sci. U.S.A. 106 (16), 6790–6795.

Greicius, M.D., Supekar, K., Menon, V., Dougherty, R.F., 2009. Resting-state functional connectivity reflects structural connectivity in the default mode network. Cereb. Cortex 19 (1), 72–78.

Hagmann, P., Sporns, O., Madan, N., Cammoun, L., Pienaar, R., Wedeen, V.J., et al., 2010. White matter maturation reshapes structural connectivity in the late developing human brain. Proc. Natl. Acad. Sci. U.S.A. 107 (44), 19067–19072.

Jackson, T., 2006. Relationships between perceived close social support and health practices within community samples of American women and men. J. Psychol. 140 (3), 229–246.

Johnston, J.M., Vaishnavi, S.N., Smyth, M.D., Zhang, D., He, B.J., Zempel, J.M., et al., 2008. Loss of resting interhemispheric functional connectivity after complete section of the corpus callosum. J. Neurosci. 28 (25), 6453–6458.

Kasprian, G., Brugger, P.C., Weber, M., Krssak, M., Krampl, E., Herold, C., et al., 2008. In utero tractography of fetal white matter development. Neuroimage 43 (2), 213–224.

Katz, L.C., Shatz, C.J., 1996. Synaptic activity and the construction of cortical circuits. Science 274 (5290), 1133–1138.

Kelly, A.M., Di Martino, A., Uddin, L.Q., Shehzad, Z., Gee, D.G., Reiss, P.T., et al., 2009. Development of anterior cingulate functional connectivity from late childhood to early adulthood. Cereb. Cortex 19 (3), 640–657.

Kostovic, I., Jovanov-Milosevic, N., 2008. Subplate zone of the human brain: historical perspective and new concepts. Coll. Antropol. 32 (Suppl. 1), 3–8.

Kostović, I., Jovanov-Milosevic, N., 2006. The development of cerebral connections during the first 20–45 weeks' gestation. Semin. Fetal Neonatal Med. 11 (6), 415–422.

Lv, Y., Margulies, D.S., Cameron Craddock, R., Long, X., Winter, B., Gierhake, D., et al., 2013. Identifying the perfusion deficit in acute stroke with resting-state functional magnetic resonance imaging. Ann. Neurol. 73 (1), 136–140.

Mailath-Pokorny, M., Kasprian, G., Mitter, C., Schopf, V., Nemec, U., Prayer, D., 2012. Magnetic resonance methods in fetal neurology. Semin. Fetal Neonatal Med. 17 (5), 278–284.

Majewska, A.K., Sur, M., 2006. Plasticity and specificity of cortical processing networks. Trends Neurosci. 29 (6), 323–329.

Murphy, K., Birn, R.M., Handwerker, D.A., Jones, T.B., Bandettini, P.A., 2009. The impact of global signal regression on resting state correlations: are anti-correlated networks introduced? Neuroimage 44 (3), 893–905.

Power, J.D., Barnes, K.A., Snyder, A.Z., Schlaggar, B.L., Petersen, S.E., 2012. Spurious but systematic correlations in functional connectivity MRI networks arise from subject motion. Neuroimage 59 (3), 2142–2154.

Power, J.D., Fair, D.A., Schlaggar, B.L., Petersen, S.E., 2010. The development of human functional brain networks. Neuron 67 (5), 735–748.

Satterthwaite, T.D., Wolf, D.H., Ruparel, K., Erus, G., Elliott, M.A., Eickhoff, S.B., et al., 2013. Heterogeneous impact of motion on fundamental patterns of developmental changes in functional connectivity during youth. Neuroimage 83, 45–57.

Schöpf, V., Kasprian, G., Brugger, P.C., Prayer, D., 2012. Watching the fetal brain at 'rest'. Int. J. Dev. Neurosci., 11–17.

Serag, A., Aljabar, P., Ball, G., Counsell, S.J., Boardman, J.P., Rutherford, M.A., et al., 2012. Construction of a consistent high-definition spatio-temporal atlas of the developing brain using adaptive kernel regression. Neuroimage 59 (3), 2255–2265.

Shattuck, D.W., Leahy, R.M., 2002. BrainSuite: an automated cortical surface identification tool. Med. Image Anal. 6 (2), 129–142.

Smith, S.M., Jenkinson, M., Woolrich, M.W., Beckmann, C.F., Behrens, T.E., Johansen-Berg, H., et al., 2004. Advances in functional and structural MR image analysis and implementation as FSL. Neuroimage 23 (Suppl. 1), S208–S219.

Smyser, C.D., Inder, T.E., Shimony, J.S., Hill, J.E., Degnan, A.J., Snyder, A.Z., et al., 2010. Longitudinal analysis of neural network development in preterm infants. Cereb. Cortex 20 (12), 2852–2862.

Stevens, M.C., Pearlson, G.D., Calhoun, V.D., 2009. Changes in the interaction of resting-state neural networks from adolescence to adulthood. Hum. Brain Mapp. 30 (8), 2356–2366.

Supekar, K., Musen, M., Menon, V., 2009. Development of large-scale functional brain networks in children. PLoS Biol. 7 (7), 15.

Takahashi, E., Folkerth, R.D., Galaburda, A.M., Grant, P.E., 2012. Emerging cerebral connectivity in the human fetal brain: an MR tractography study. Cereb. Cortex 22 (2), 455–464.

Thomason, M.E., Brown, J.A., Dassanayake, M.T., Shastri, R., Marusak, H.A., Hernandez-Andrade, E., et al., 2014. Intrinsic functional brain architecture derived from graph theoretical analysis in the human fetus. PLoS ONE.

Thomason, M.E., Dassanayake, M.T., Shen, S., Katkuri, Y., Alexis, M., Anderson, A.L., et al., 2013. Cross-hemispheric functional connectivity in the human fetal brain. Sci. Transl. Med. 5 (173).

Van Dijk, K.R., Sabuncu, M.R., Buckner, R.L., 2012. The influence of head motion on intrinsic functional connectivity MRI. Neuroimage 59 (1), 431–438.

Vincent, J.L., Patel, G.H., Fox, M.D., Snyder, A.Z., Baker, J.T., Van Essen, D.C., et al., 2007. Intrinsic functional architecture in the anaesthetized monkey brain. Nature 447 (7140), 83–86.

Weissenbacher, A., Kasess, C., Gerstl, F., Lanzenberger, R., Moser, E., Windischberger, C., 2009. Correlations and anticorrelations in resting-state functional connectivity MRI: a quantitative comparison of preprocessing strategies. Neuroimage 47 (4), 1408–1416.

Whitfield-Gabrieli, S., Nieto Castanon, A., 2012. Conn: a functional connectivity toolbox for correlated and anticorrelated brain networks. Brain Connect.